PROCEEDINGS, TOUGH Symposium 2006
Lawrence Berkeley National Laboratory, Berkeley, California, May 15–17, 2006

ASCATA—A TOUGH2 BASED PROGRAM FOR AUTOMATED SIMULATION OF COMPRESSED AIR TUNNEL ADVANCE

Gerhard Steger and Stephan Semprich

Institute for Soil Mechanics and Foundation Engineering, Graz University of Technology
Rechbauerstraße 12
8010 Graz, Austria
e-mail: gerhard.steger@tugraz.at

ABSTRACT

In compressed air tunneling an excess air pressure is applied inside the tunnel to prevent groundwater-inflow. Due to the excess pressure compressed air partly penetrates into the surrounding ground. The costs for the continuous generation of the compressed air may reach a significant share of the total tunnel construction costs. Especially contractors are therefore interested in predictions of the expected air losses to determine the capacity of the air supply equipment on site and to estimate the energy costs for the generation of the compressed air. Consulting engineers want to know how the escaping air influences surface settlements and tunnel face stability.

ASCATA—a TOUGH2 based program, was developed in order to compute the transient air flow rates during the tunnel advance and to simulate the effects of the escaping compressed air to the ground. TOUGH2 was chosen as core of the new program because of the available flow module EOS3 (active air and water flow) and the open source code which, among other things, allowed for the implementation of an automatic advance sequence.

Initially, an introduction of tunneling under compressed air is given in the paper. In the following, the main features of the developed program are described. Special attention is given to the algorithms which are used for the automatic advance simulation. The functionality of the program is demonstrated by two case studies.

INTRODUCTION

Tunneling Under Compressed Air

Compressed air is a frequently used and well proven auxiliary method in urban tunneling in groundwater bearing soils. An excess air pressure is applied inside the tunnel to prevent groundwater inflow. For this purpose, a bulkhead situated close to the tunnel portal separates the excavation area from the atmosphere. Compressed air is then pumped into the tunnel via compressors. People, machinery and construction materials have to enter and leave the tunnel through an air lock.

Compressed air may be used in combination with the NATM (New Austrian Tunneling Method), the top-cover method or shield tunneling. Advantages of this method of groundwater control among others include a high efficiency in appropriate ground conditions and the environmentally sound nature of the use of compressed air.

The magnitude of the applied air pressure p_a is adjusted to the hydrostatic pressure p_w at the tunnel base. Due to the negligible low gravity potential, the air pressure is virtually constant over the height of the tunnel whereas the water pressure increases linearly. As a consequence, an unavoidable pressure difference $\Delta p = (p_a - p_w)$ acts on the tunnel walls. This pressure difference is 0 at the base of the tunnel ($\Delta p_b = 0$), and reaches its maximum at the top of the tunnel. For NATM-tunnels the maximum Δp is given by the diameter of the tunnel d and the unit weight of water ($\Delta p_{top} = d \cdot \gamma_w$) and for top-cover tunnels by the depth of the invert beneath the groundwater-table and the unit weight of water ($\Delta p_{top} = t_b \cdot \gamma_w$), see Figure 1.

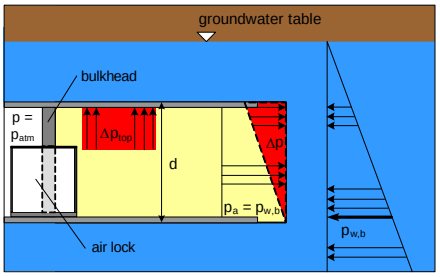

a) Longitudinal tunnel section

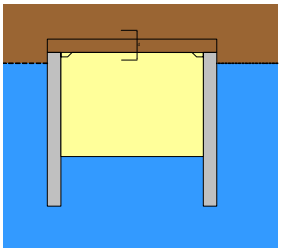

b) Cross sections

Figure 1. Pressure difference Δp on the boundaries of a NATM- and a top-cover tunnel.

The described pressure difference represents a driving potential which induces an air flow from the tunnel into the surrounding ground. These air losses have to be replaced continuously, so as to maintain the necessary excess air pressure inside the tunnel.

In NATM tunneling air losses q_a take place both through the unsupported tunnel face and through cracks and gaps of the shotcrete lining, see Figure 1b, left. The NATM in combination with compressed air is mainly used in sandy and silty soils. If used in pebbly soils grouting is necessary to reduce the air permeability of the ground.

In the top-cover method, the tunnel consists of the lateral bore-pile or diaphragm walls and the top concrete slab, similar to an upside-down box. Air losses only take place through gaps and cracks of the lateral tunnel walls because the top concrete slab is practically impermeable, see Figure 1b, right. The application of this method is not limited by the soil permeability as the excavation area is completely enclosed by structural elements.

Motivation for Research

Contractor interests

For contractors, it is important to estimate correctly the maximum air flow rate q [m³/min] and the total amount of air losses Q [m³] to evaluate the capacity of the air supply equipment and the energy costs of the generation of the compressed air respectively.

In compressed air tunneling flow rates higher than 600 m³/min have been reported (Kramer and Semprich, 1989). That implied total air losses of more than 100,000,000 m³ for single tunneling projects. The resulting costs for the generation of the compressed air reached several thousand Euros per m tunnel advance.

In the past and current engineering practice, the prediction of air losses is based on semi-empirical relationships (e.g. Kramer and Semprich, 1989). In many cases these simplified methods were not capable of predicting air losses accurately resulting in economic failure of the tunneling project. By employing 3d-numerical multiphase flow simulation methods significant improvements on the accuracy of predicting air losses can be gained (Steger et al., 2005).

Consulting engineers interests

To accurately compute surface settlements and tunnel face stability, consulting engineers have to consider the effects of the escaping compressed air to the ground. Coupled hydro-mechanical simulations are needed for this purpose.

The escaping air is penetrating into originally saturated soil around the tunnel excavation area. As the out-flowing air is under excess pressure, the pore pressures around the tunnel are raised. Further, the escaping air is partly replacing the pore water. As a consequence the soil gets unsaturated and capillary pressures develop.

These two effects of the compressed air flow are working in opposition. While the increase of pore pressures reduces the effective stress in the soil, the developing capillary pressures are increasing it. It is therefore not possible to assess *a priori* how surface settlements are influenced by the air losses.

This paper focuses on the numerical simulation of air losses but the developed program has also already been used in a coupled hydro-mechanical simulation (Chinkulkijniwat, 2005) of a tunnel advance.

NUMERICAL SIMULATION OF COMPRESSED AIR TUNNEL ADVANCE

General

The flow problem to be dealt with in compressed air tunneling is a transient two phase flow of water and air. Air is the active phase which is forcing out water of the soil pores. Most of the available geotechnical software is only capable simulating flow in unsaturated conditions with the air phase considered as a passive bystander. Obviously, this type of software is not suitable for numerical simulation in compressed air tunneling.

The multiphase flow simulator TOUGH2 (Pruess et al., 1999) was chosen to develop a numerical tool to simulate the air losses during the driving of compressed air tunnels. To ensure a maximum of convenience and time efficiency for the advance simulations, an automatic advance sequence and an integrated evaluation of the air flow rates were programmed and combined with TOUGH2. For model development, the TOUGH2 pre- and postprocessor PetraSim (RockWare Inc.) is used.

Numerical Base Model

In the numerical base model the ground conditions over the whole advance length are modeled, while only the starting point of the tunnel advance under compressed air is modeled. Due to symmetry, only half of the cross section is considered. For convenience the following description refers to a model for a NATM-tunnel but the principles for top-cover tunnels are the same. The concept of the described model has first been used by Scheid (2003).

To the soil grid blocks of the model (see Figure 2) a hydrostatic pressure distribution and a liquid satura-

tion of S_l = 0.99 are assigned as initial conditions. To describe the relative permeability of the liquid phase the van Genuchten-Mualem model (1976; 1980) is used. For the gas phase the Corey (1954) relative permeability function and experimentally defined functions (Steger et al., 2005) are employed, depending on the soil types modeled. The capillary pressures are taken into account with the van Genuchten function (1980).

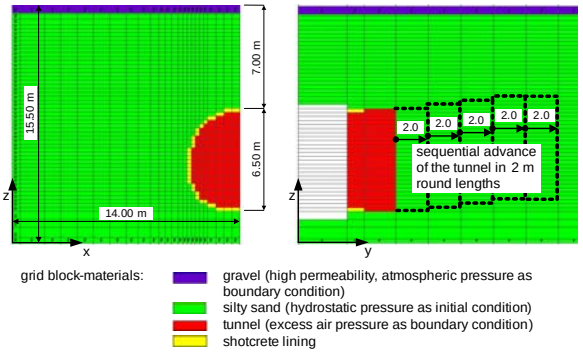

Figure 2. Example of a numerical base model for a tunnel advance simulation

The excess air pressure inside the tunnel (limited to 3.6 bars due to negative health impact on workers) is modeled with a Dirichlet-boundary condition. Perfect gas mobility and zero water permeability are assigned to this grid blocks. The magnitude of the assigned gas pressure is according to the hydrostatic water pressure at the tunnel base.

The shotcrete lining is modeled with a linear relative permeability function for both liquid and gas phase, and an intrinsic permeability of $K_i = 5 \cdot 10^{-14}$ m² is assigned. No capillary pressure function is assigned.

The top boundary of the model represents the atmosphere or in certain cases a soil layer above the groundwater level with high permeability. An assigned Dirichlet- boundary condition ensures a constant pressure of 100 kPa.

Table 1. Material properties

material	RP-function	CP-function	boundary condidtion
soil (all soil types)	van Genuchten-Mualem; Corey& others	van Genuchten	only at model boundary
tunnel (= excess air pressure)	gas perfectly mobile	-	Dirichlet (p_g < 360 kPa)
shotcrete	linear	-	-
atmosphere	all phases perfectly mobile	van Genuchten	Dirichlet (p_g = 100 kPa)

The bottom, the left lateral boundary and back side boundary are also simulated with Dirichlet-conditions, keeping the initial hydrostatic pressure distribution and the initial water saturation of 99 % constant. To the front and the right lateral boundary (symmetry plane) a Neumann-condition with zero flux is assigned. The simulations are done assuming isothermal conditions with a temperature of 10° C.

Modeling the Tunnel Advance

The advance of NATM-tunnels is cyclic, consisting of a sequence of excavation and placing a reinforced shotcrete layer as primary support to the tunnel lining. In a similar manner the numerical simulation of the tunnel advance is done.

The tunnel advance is simulated in 2 m round lengths, as shown in Figure 2. For this purpose soil grid blocks behind the tunnel face have to be replaced sequentially by tunnel-grid blocks. At the same time the tunnel grid blocks along the perimeter of the tunnel ahead of the tunnel face have to be replaced by shotcrete-grid blocks, see Figure 3.

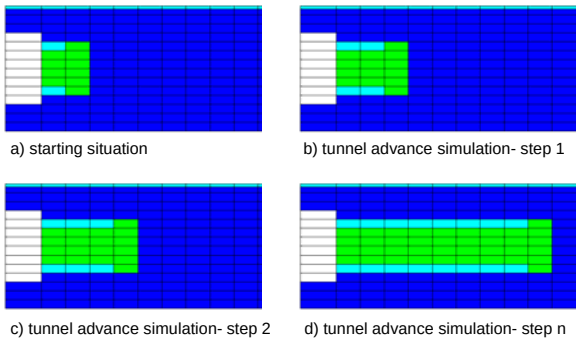

Figure 3. Principle of tunnel advance simulations

Between each step a flow simulation with duration depending on the advance velocity is conducted. The thermodynamic state of the model at the end of each advance step is the initial condition for the subsequent advance step. This procedure has to be repeated until the full advance length is reached. In the course of the advance simulation the air flow rates of all flow connections between tunnel grid blocks and soil grid blocks as well as between tunnel grid blocks and shotcrete grid blocks are evaluated.

THE PROGRAM ASCATA

General Structure

From the description of modeling of the tunnel advance it can be seen that such a simulation is a series of flow computations with input-files of models adapted to the ongoing tunnel advance. Acknowledging this fact, the program ASCATA (**A**utomatic **S**imulation of **C**ompressed **A**ir **T**unnel **A**dvance) is built up around a modified and enhanced TOUGH2 code using the EOS3 flow module, see Figure 3.

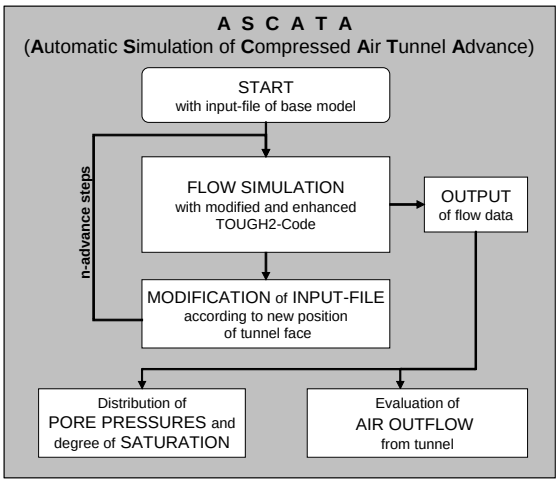

Figure 4. Simplified flow chart of ASCATA

The key task of ASCATA is therefore to create a new input-file according to the new position of the tunnel face after each flow computation and carrying out n-advance steps according to the desired length of the tunnel. To carry out a series of consecutive computations can simply be achieved by implementing a loop into the main TOUGH2-file T2CG1. For relocating the tunnel face and to allow an integrated air flow data evaluation, several modifications need to be done in the ELEME-, CONNE-, INCON- and COFT-block of the input-file.

To meet these requirements a main subroutine "input-new" and several sub-subroutines were added to the TOUGH2-files. Beyond, major and minor changes have to be done throughout the original TOUGH2-code to ensure compatibility of all routines.

The subroutine "input-new"

The main task of this subroutine is to adapt geometrically the input-file to the progress of the tunnel advance to relocate the tunnel face layer by layer to increase the length of the tunnel. This means that for the concerned grid blocks the assignment of material properties and thermodynamic conditions have to be changed. The key problem in this context is to identify the numbers of these grid blocks. To achieve this, a special tunnel-advance algorithm is implemented in the subroutine "input-new". The thermodynamic state of the model for the new input-file can simply be adopted from the SAVE-file of each TOUGH2-computation.

As basis for the tunnel-advance simulation, the arrays with the numbers of all tunnel grid blocks at the tunnel face ($\boldsymbol{V}_{TuF}$) and the ring of shotcrete grid blocks immediately behind ($\boldsymbol{V}_{ScF}$) are used. The numbers of these grid blocks are identified by the subroutine "tunnel face" (see below).

Before developing the advance algorithm, the way PetraSim assigns the grid block numbers had to be determined. It has been found that PetraSim numbers first along the x-direction, then along the y-direction and finally along the z-axis. The numbering is done in rows.

Consider a model which has E_x layers in *x*-, E_y layers in *y*- and E_z layers in z-direction. From the described numbering preferences of PetraSim it can be derived that the number of a grid block N which is in the same row but at a distance of m_i layers of grid blocks in the *x*-direction to a reference grid block N_G can be computed by $N = N_G + 1 \cdot m_x$, in y-direction by $N = N_G + E_x \cdot m_y$, and in z-direction by $N = N_G + (E_x \cdot E_y) \cdot m_z$.

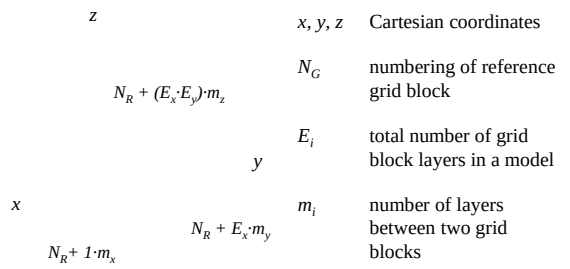

Figure 5. PetraSim grid block numbering

For any arbitrarily situated grid block in any model the number can be computed by a combination of these three relationships:

$$N = N_G + 1 \cdot m_x + E_x \cdot m_y + (E_x \cdot E_y) \cdot m_z \qquad (1)$$

For ASCATA-simulations the y-axis is chosen as the advance direction. It is not necessary to simulate a horizontal curvature of the tunnel because it has no influence to the flow computation. Hence, changes of grid block numbers in x-direction can be excluded.

Suppose that the reference grid block is now the array $\boldsymbol{V}_{TuF}$ containing the numbers of the tunnel grid blocks at the tunnel face $N_{\boldsymbol{TuF,i}}$ of the numerical base model. The number of every soil grid block one layer behind the tunnel face which has to be changed into tunnel elements can then be computed with

$$N_i = N_{TuF,i} + E_x \cdot 1, \qquad (2)$$

and for the *n*-th tunnel-advance step with

$$N_i = N_{\boldsymbol{TuF,i}} + E_x \cdot n. \qquad (3)$$

Because it is of special interest to simulate tunnel advances with varying gradients, also the position of the tunnel face in vertical *z*-direction has to be altered (see Figure 2). The number of layers m_t by which the tunnel advance has to be displaced can be calculated by means of the gradient of the tunnel and the *z*-center point distances between the layers. The final

equation to compute the number of the grid blocks to be modified is:

$$N_i = N_{\boldsymbol{TuF,i}} + E_x \cdot n + (E_x \cdot E_y) \cdot m_t \qquad (4)$$

The advance step n and the function of the gradient m are working as variables. At every advance step, the subroutine "new input" compares each grid block number from the input file with all numbers that can be computed with the algorithm, using concurrently n and m_t. If for any grid block conformity is found that means that for the next advance step this grid block has to be modified from a soil grid block to a tunnel grid block, see Figure 6.

In the ELEME-block:

```
Do I = 1, k

        if [EL  = V_TuF(I)  + E_x·n + (E_x· E_y)·m_t] then
                MAT = TUNEL
                VOL = VOL · 10^50

        endif

Enddo
```

In the INCON-block:

```
Do I = 1, k

        if [EL  = V_TuF(I)  + E_x·n + (E_x· E_y)·m_t] then
                X1 = P + T · 10000
                X2 = 0.99
                X3 = X3

        endif

Enddo
```

k	*total number of tunnel grid blocks at tunnel face*
P	*applied air pressure inside the tunnel [pa]*
I	*control variable*
MAT	*material code name*
VOL	*grid block volume*
X1, X2, X3	*primary variables (pressure, gas saturation, temperature)*
T	*a function computing the depth of the tunnel base*

Figure 6. Schematic code details of the subroutine "input-new"

In the ELEME-block the material labeling of the concerned grid blocks is changed to "TUNEL". Tunnel grid blocks are simulating the excess air pressure inside the tunnel and therefore represent a Dirichlet-boundary condition. To achieve this, the volume of the grid block is simply multiplied by a factor of 1E50, see Figure 6.

In the INCON-block the gas pressure has to be raised according to the magnitude of the hydrostatic pressure at the base of the tunnel. If the tunnel is inclined the gas pressure is a function of the depth of the tunnel face below the ground-water table and is calculated by a function T for each advance step. Further the gas saturation is raised to 0.99.

After all these changes have been carried out, the next flow simulation can be started. This procedure of modifying the input-file and subsequent flow computation is repeated until the tunnel has reached the desired length.

The subroutine "flow-data"

In the course of the advance simulation the total air-outflow from the tunnel has to be evaluated. For longer tunnels thousands of grid block interfaces have to be identified and the air flow data of the single connections have to be summed up to receive the total air flow rate. To better analyze the air losses it is of interest to evaluate them for the unsupported tunnel face and for the shotcrete lining separately.

The subroutine "flow-data" searches the CONNE-block of the input-file for tunnel-soil (at the tunnel face) and tunnel-shotcrete (at the tunnel lining) grid block interfaces. Then the identified connections are written in the COFT-block. The size of the array where TOUGH2 is storing these data had to be increased from 50 to 5000. The air and water flow data of the listed connections are printed in the COFT-file after each TOUGH2-simulation. From here the air-flow data are summed up to get the air losses. The computed mass flow M_g is finally converted in a volume flow V_g by employing the ideal gas equation:

$$V_g = M_g \frac{RT}{\omega \cdot p_g} \qquad (5)$$

R is the gas constant, T the absolute temperature, ω the molecular mass of air and p_g the gas pressure.

Identification of tunnel-shotcrete connections

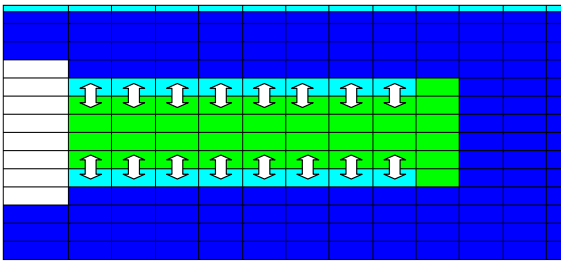

Figure 7. Tunnel-shotcrete flow connections (schematic)

In order to enable the subroutine to identify these connection data, first all numbers of tunnel and shot-crete grid-blocks have to be known. For this purpose the ELEME-block of the input-file is searched for "TUNEL" and "SHOTC" labeled grid blocks. The corresponding numbers are stored in the two arrays $\boldsymbol{V}_{Tu}$ and $\boldsymbol{V}_{Sc}$ respectively.

With this data, the CONNE-block is checked for the sought connections in the next step. If the first part of the connection labeling does neither correspond to a

tunnel nor to a shotcrete grid block number, the connection is not searched for and the program will check the next connection. In case the first part corresponds to a tunnel or to a shotcrete grid-block number, it is possibly a searched-for connection. In this case, the second part of the connection will also be checked. If either the first number corresponds to a tunnel grid block and the second number corresponds to a shotcrete grid block or the first number corresponds to a shotcrete grid block and the second number corresponds to a tunnel grid block, the connection is a searched-for one. In this way all the connections of the CONNE-block are screened and the identified ones are stored in the array ***TSCON*** and then listed in the COFT-block.

In the program this procedure was realized with four if-conditions within four loops, where the number of cycles depends on the size of the tunnel- ($\boldsymbol{V}_{Tu}$) and shotcrete arrays ($\boldsymbol{V}_{Sc}$) respectively, see Figure 8.

```
10      read (EL1, EL2)

        do I = 1, s
                if (EL1 = V_Sp (I)) goto 100
        enddo

        goto 200

100     do I = 1, r
                if (EL2 = V_Tu(I)) then
                        J = J + 1
                        TSCON(J) = (EL1, EL2)
                        goto 10
                endif
        enddo

200     do I = 1, r
                if (EL1) = V_Tu(I)) goto 300
        enddo

        goto 10

300     do I =1, s
                if (EL2 = V_Sp (I)) then
                        J = J + 1
                         TSCON(J) = (EL1, EL2)
                         goto 10
                 endif
        enddo

        goto 10
```

EL1, EL2	*grid block numbers (defining a grid connection)*
I, J	*control variables*
V_{Sp}, V_{Tu}	*vectors containing all tunnel respectively shotcrete grid blocks*
r, s	*total number of tunnel respectively shotcrete grid blocks*
TSCON	*array to store the identified connections*

Figure 8. Schematic code details of the subroutine "flow-data" (part a)

Identification of tunnel-soil connections

The connections searched for are characterized by one part being a tunnel grid block and the other part being a soil grid block. For this condition all the connections of the CONNE-block have to be checked.

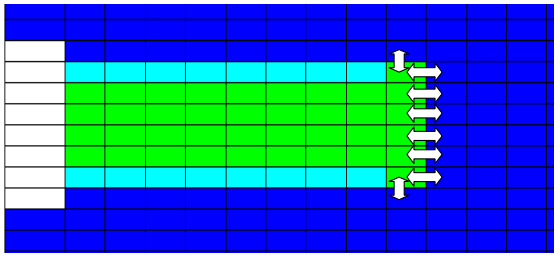

Figure 9. Tunnel-soil flow connections (schematic)

Even though the array with the numbers of all tunnel grid blocks is already known, it is not advisable to use the same strategy here as for the identification of the tunnel-shotcrete connections. If the same procedure would be used, a second array containing all soil grid blocks would have to be created to check identity with the connection numbers. As the used models usually have between 10,000 and 50,000 grid blocks, a very long computation time would be the consequence. It has therefore been decided to use a procedure which is based on conformity and exclusion principles.

Each connection will first be checked to see if either the first or the second part is conforming to a tunnel grid block. Additionally, the remaining part must not be another tunnel grid block or a shotcrete grid block. If this condition is fulfilled, the connection must be a searched-for tunnel-soil connection that will be stored and later be listed in the COFT-block.

In the subroutine (see Figure 10), each connection is first checked to see if neither one of the numbers marking the connection is a shotcrete grid block. If this is not the case, it is further checked if either the first or the second numbers is characterizing a tunnel grid block. If not, the considered connection is between two soil grid blocks and not of interest here. Again a new connection will be read in.

If none of the numbers is marking a shotcrete grid block, but one part of the connection has been identified as a tunnel grid block, the connection is possibly a searched-for one. The last thing to be controlled is that not both numbers belong to tunnel grid blocks. If this last condition is fulfilled, all other possible connection types than the searched-for tunnel-soil connections have been excluded. The one identified in this way is stored in the array ***TFCON*** and later listed in the COFT-block of the input-file.

```
10          read EL1, EL2

100         do I = 1, s
                        if (EL1 = V_Sc(I)) goto 10
                        if (EL2 = V_Sc(I)) goto 10
            enddo

200         do I = 1, r
                        if (EL1 = V_Tu(I)) goto 400
            enddo

300         do I = 1, r
                        if (EL2 = VTu(I)) goto 500
            enddo

            goto 10

400         do I = 1, r
                        if (EL2 = V_Tu(I)) goto 10

                            j = j+1
                           TFCON(J) = EL1, EL2
                            goto 10

                        endif

            enddo

 500        do I = 1, r
                        if (EL1 = VTu(I)) goto 10

                            j = j+1
                            TFCON(J) = EL1, EL2
                           goto 10

                        endif

              enddo
```

EL1, EL2	*grid block numbers (defining a connection)*
I	*control variable*
j	*counter variable*
V_{Tu}, V_{Sc}	*vectors containing all tunnel and shotcrete grid blocks respectively*
r, S	*total number of tunnel and shotcrete grid blocks respectively*
E_x, E_y	*total number of grid block layers in x- and y-direction*
TFCON	*array to save the identified tunnel face-soil connections*

Figure 10. Schematic code details of the subroutine "flow-data" (part b)

The subroutine "tunnel face"

For the simulation of the tunnel advance with the presented algorithm, the tunnel grid block numbers $\boldsymbol{N_{TuF,i}}$ directly situated at the tunnel face have to be known (see subroutine "input-new"). If the modeled tunnel section in the base model consists of two or more grid block layers, a special procedure is required to identify these grid blocks. For this purpose the subroutine "tunnel face" has been programmed.

In the first step, again, all tunnel grid blocks in the input-file are identified by searching the ELEME-block for "TUNEL" material assignments and stored in the array $\boldsymbol{V_{Tu}}$. The problem now is to filter out of these tunnel grid blocks only the ones which are situated at the tunnel face. The idea is to determine first a second array $\boldsymbol{V_{xz}}$ which contains all numbers of grid blocks of the vertical *x*-*z*-layer that includes the tunnel face. By identifying the common elements of both arrays the searched for tunnel grid blocks at the tunnel face can be determined, see Figure 11.

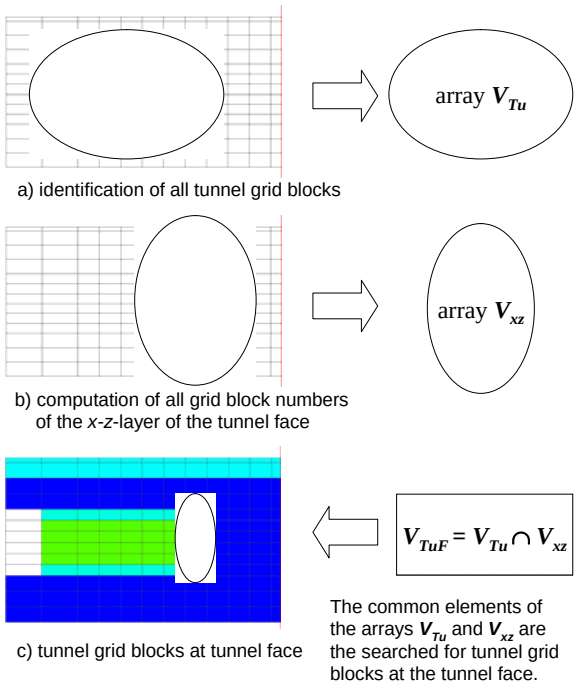

Figure 11. Workings of the subroutine "tunnel face"

This second array $\boldsymbol{V_{xz}}$ can be computed by considering the numbering mode of PetraSim. The grid blocks have an increasing number in *y*-direction which is also the advance direction. It can therefore be concluded that the tunnel grid block with the highest numbering is situated at the tunnel face. By knowing the total number of grid blocks layers E_x in *x*, E_y in *y*- and E_z in z-direction, the position n_y of the *x*-*z*-layer where this tunnel grid block is situated can be detected. An algorithm to compute all grid blocks of this layer can now be derived by using a double loop, see the schematic code details in Figure 12.

```
Do I = 1, (E_z -1)

                do K = 1, E_x

                        j = j + 1

                        VTUxz (j) = Ex * Ey * k + ny * Ex + K

                enddo

Enddo
```

Ex, Ey	*total number of grid block layers in x- and y-direction respectively*
ny	*position of tunnel face grid block layer*
VTUxz	*array with computed numbers of the x-z-tunnel face grid block layer*
I, K	*control variables*

Figure 12. Schematic code details of the subroutine "tunnel face" (part a)

After this second array $\boldsymbol{V_{xz}}$ is computed, its elements are compared with all of the elements of the tunnel grid block array. In the subroutine this is again done by means of a double loop. While one grid block number of the first array is kept fixed, it is compared with all elements of the second array. If two elements are matching, the grid block number will be stored in the array ***TuF.*** If there is no matching, the next element of the first array will be compared with all elements of the second array, see Figure 13.

```
Do I = 1, r
        do K = 1, t
            if (VTu ( I ) = V2 ( J )) then
                j = j + 1
                VTuF (K) = VTu( I )
            endif
        enddo
Enddo
```

VTu	*array containing all numbers of tunnel grid blocks*
Vxz	*array containing all numbers of grid blocks of the x-z-layer of the tunnel face*
VTuF	*computed array containing all numbers of tunnel grid blocks situated at the tunnel face*
r	*total number of tunnel grid blocks*
t	*total number of grid blocks of the x-z-layer*
j	*counter variable*
I, K	*control variables*

Figure 13. Schematic code details of the subroutine "tunnel face" (part b)

INVESTIGATION OF AIR LOSSES IN NATM-TUNNELING

Soil and shotcrete properties

In the following tunnel advance simulations the ground was assumed to be homogeneous, consisting of a slightly silty sand with a saturated water permeability $k_w = 5 \times 10^{-5}$ m/s and a porosity $n = 0.35$.

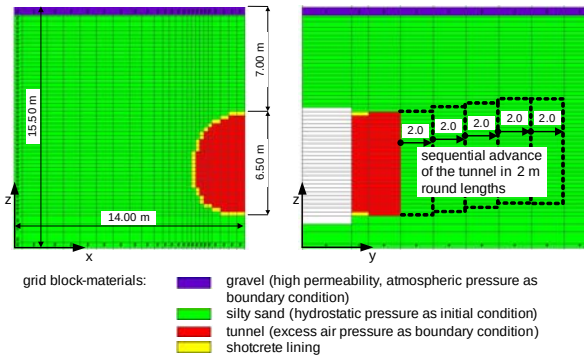

Figure 14. Base model for the simulation of a NATM-tunnel advance.

The unsaturated conductivity parameters (see Table 2) were estimated from the grain-size distribution, based on a non-linear regression analysis. As characteristic values, an *m*-value of 0.65 and an air entry value p_0 of 3.75 kPa have been computed. To the shotcrete an intrinsic permeability of $K_i = 7.0 \times 10^{-14}$ m² based on laboratory tests of Kammerer (2000) was assigned. The relative permeability-saturation behavior was taken into account with a linear relationship.

Table 2. Grain size distribution and fluid conductivity parameters.

Mass fractions [%]	*Cl*	*Si*	*FSa*	*MSa*	*CSa*
	0	5	45	45	5
Unsaturated conductivity parameters	S_{lr}	S_{ls}	S_{gr}	*m [-]*	p_0 *[kPa]*
	0.10	1.0	0.10	0.65	3.75
Intrinsic permeability K_i (fluid independent):	$6.7 \cdot 10^{-12}$ m²				
Water permeability $k_{w,100}$ at S_w = 100%:	$5.0 \cdot 10^{-5}$ m/s				
Air permeability $k_{g,100}$ at S_g = 100%:	$3.5 \cdot 10^{-3}$ m/s				

The influence of a varying gradient

In former studies (Steger and Semprich, 2005) the influence of different but constant overburdens on the air losses of horizontally driven tunnels has been investigated. It has been found that the air losses through the tunnel face remain more or less constant, whereas there is a 25 % increase of the air losses through the shotcrete lining when results of tunnel advance simulations 2.0 m and 5.0 m below the groundwater table are compared to each other.

Provided with the data from these simulations, in a next step the air losses are investigated for a 100-m-long tunnel with three different gradient-sections. The cross section of the tunnel is mouth-shaped, with an average diameter of 6.50 m, see Figure 3. The modeled cross section corresponds to a typical single-track subway tunnel in Vienna. The thickness of the primary applied shotcrete lining is 25 cm.

In the first simulation the tunnel excavation starts horizontally with an overburden of 2 m (with respect to the ground-water table). After 30 m of advance, the gradient changes to -10.0 % for the next 30 m. The remaining 40 m are again driven horizontally at an overburden of 5.0 m, as depicted in Figure 15. The described geometry was chosen to receive expressive trends. The necessary excess air pressure has to be increased continuously from first 85 kPa to finally 115 kPa, according to the pore-water pressure at the tunnel base. An advance velocity of 5 m/d is assigned.

In Figure 15, the computed results are shown separately for the air losses through the shotcrete lining and the tunnel face, and also the total air losses as a sum of both is depicted (thick light grey graph). The discontinuities appearing in the graphs are due to the discrete simulation of the tunnel advance.

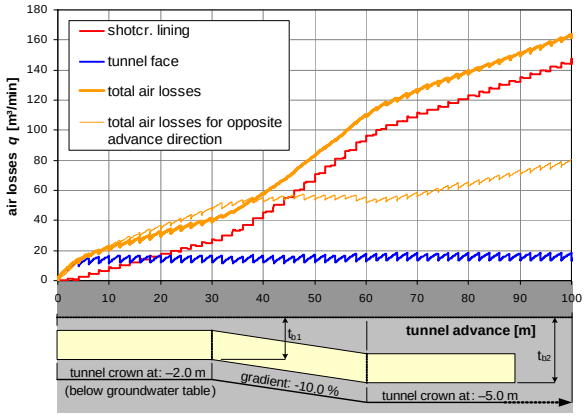

Figure 15. Computed air losses for a NATM-tunnel with varying overburden.

It can be seen that the air losses through the tunnel face with about 18 m³/min remain more or less constant over the whole advance length, as could be predicted from the before mentioned horizontal advance simulations. The strongly inclined graph within each 2 m round length indicates the transient nature of the air losses. A lower advance rate would therefore lead to a higher air flow rate and vice versa.

The air losses through the shotcrete lining are increasing continuously with the ongoing length of tunnel excavation. An exceptionally strong increase of 2.57 m³/min per m can be observed during the advance of the tunnel in the inclined section, whereas in the horizontal sections there is an increase of 0.89 resp. 1.12 m³/min. The total air losses at the end of the 100 m tunnel advance reach 165 m³/min.

The second simulation is carried out exactly the opposite way round (geometry not depicted in Figure 4). The tunnel advance starts horizontally with 5.0 m overburden, then has a gradient of +10 % for the next 30 m and ends again horizontally with an overburden of 2.0 m. For a better overview, only the total air losses are depicted in Figure 15 (thin light grey graph). The air losses through the tunnel face are consequently the same as before. Also as before, the air losses through the shotcrete lining show a remarkable change during the advance in the inclined section, but this time a decrease can be observed, though the increasing length of the tunnel.

The reason for this extraordinary performance is that during the advance in the inclined section the air pressure in the tunnel has to be increased or decreased continuously, according to the hydrostatic pressure at the base of the tunnel face. Therefore, at the tunnel face the maximum pressure difference is always $\Delta p = (d \cdot \gamma_w)$, as shown in Figure 1. But in the tunnel sections situated behind, where the same air but different water pressure acts, the pressure difference is variable.

For the first simulation, it increases to finally $\Delta p = [(d \cdot \gamma_w) + (t_{b2} - t_{b1}) \cdot \gamma_w]$, causing the strong increase of air losses. The contrary occurs if the tunnel is driven from the opposite direction, the pressure difference in the deeper located, behind sections is reducing to $\Delta p = [(d \cdot \gamma_w) - (t_{b2} - t_{b1}) \cdot \gamma_w]$. Once the advance is horizontal again, the air losses show a normal behavior again.

The maximum total air losses are 165 m³/min and 80 m³/min respectively for the two different advance simulations. These results are pointing out that it is always favorable to drive compressed air tunnels in the direction of decreasing overburden, so that the air pressure can be reduced during the advance. For the first simulation, the total amount of air losses is approximately 2,450,000 m³ and for the second 1,450,000 m³. This means a possible saving of 41 % of the energy costs for the generation of the compressed air.

INVESTIGATION OF AIR LOSSES IN TOP-COVER TUNNELING

Situation, soil and material properties

In Figure 16 the numerical model of the cross section is depicted. The tunnel excavation has a width of 13.5 m and a height of 10.0 m, and the cover fill is 2.0 m. The bore-pile walls are modeled with an effective thickness of 0.60 m. The groundwater table is located 0.50 m below the lower edge of the top slab. The necessary excess air pressure is 95 kPa.

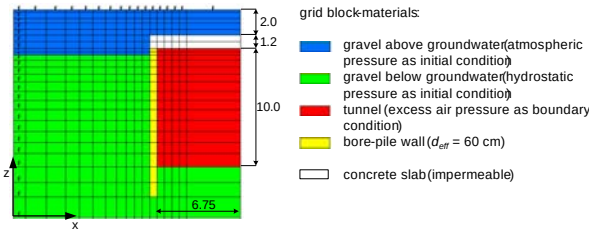

Figure 16. Cross section of the numerical model for the top-cover tunnel

The tunnel is situated in a homogeneous sandy gravel layer with a saturated permeability $k_w = 5 \times 10^{-4}$ m/s and a porosity $n = 0.35$. The RP-function is chosen as before, only the residual water saturation $S_{w,r}$ and the m-value were changed to 0.05 and 0.80 respectively, because of the coarseness of gravel. For the same reason, no capillary pressure-function was assigned.

An intrinsic permeability of $K_i = 3.0 \times 10^{-14}$ m² was assigned to the bore-pile wall, again based on laboratory tests of Kammerer (2000) and empirical considerations (material imperfections etc.). The relative permeability-saturation behavior was taken into account with a linear relationship.

The influence of bulkheads

Two advance simulations of a 300 m long top-cover tunnel are conducted. In the first simulation bulkheads are situated only at the beginning and at the end of the tunnel. In the second case two additional bulkheads are situated 100 and 200 m from the starting point of the tunnel advance, thus dividing it into three 100-m-long sections. The assigned advance velocity is 5 m/d.

The calculated results of the first case are shown in Figure 6. The air losses differed in the excavated section and behind the “tunnel face”. The air flow through the bore-pile wall in the excavated section is increasing linearly with the ongoing tunnel advance. The air flow through the “tunnel face” from 150 m to 300 m tunnel advance reduces gradually to almost zero. This occurs because the further extension of the flow field in the longitudinal direction is hindered by the bulkhead at the end of the tunnel. The air losses reach a maximum value of 98 m³/min.

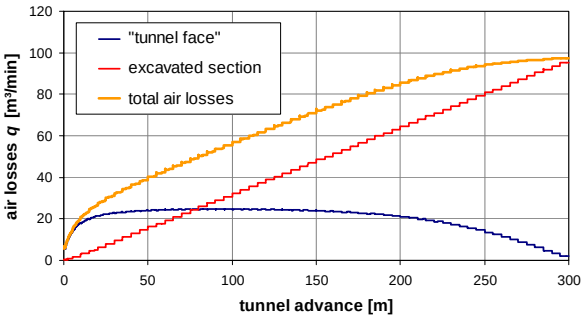

Figure 17. Computed air losses for a top-cover tunnel without intermediate bulkheads

The results of the second simulation are shown in Figure 17. Obviously there is no change of the air losses occurring in the excavated section. In the longitudinal direction the air flow varies between 18 and 2 m³/min due to the presence of the two additional bulk heads. At the end of the 300 m tunnel advance the rate of air flow is 98 m³/min, the same as before. It can be seen that the amount of compressed air which can be saved due to the additional bulkheads is relatively low (less than 10 %).

It is noted that the conducted simulations base on the assumption that the construction joint between the bore-piles and the top slab is airtight. Furthermore, in higher permeable soils intermediate bulkheads are more effective to reduce air losses because the flow field will extend stronger in longitudinal direction.

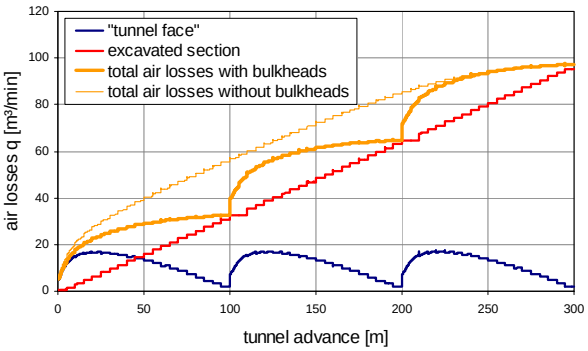

Figure 18. Computed air losses for a top-cover tunnel with intermediate bulkheads

SUMMARY AND CONCLUSIONS

3-D numerical simulation of air losses allows detailed consideration of unsaturated fluid conductivity. Furthermore it is important to simulate the advance of the tunnel as the air flow is transient and therefore depends on the advance velocity. According to these demands, the program ASCATA has been developed. The conducted case studies show a significant influence of a varying gradient of a NATM driven tunnel on the air losses. In order to reduce air losses it is favorable to drive the tunnel towards the direction of increasing overburden. For tunnels constructed in top-cover technique, intermediate bulkheads show only a low efficiency to reduce to air losses.

REFERENCES

Chinkulkijniwat, A., Multiphase flow in Unsaturated Soils and the Induced Deformation with Respect to Compressed Air Tunneling, *Mitteilungshefte Gruppe Geotechnik Graz*, Graz University of Technology, 8, 2000.

Corey, A.T., The interrelation between oil and gas relative permeabilities, *Producers monthly*, 38-41, November 1954.

van Genuchten, M.Th., A Closed-form Equation for Predicting the Hydraulic Conductivity of Unsaturated Soils, *Soil Sci. Soc. of America*, 44(5), 892-898, 1980.

Kammerer, G., Experimentelle Untersuchungen von Strömungsvorgängen in teilgesättigten Böden und in Spritzbetonrissen im Hinblick auf den Einsatz von Druckluft zur Wasserhaltung im Tunnelbau, *Mitteilungshefte Gruppe Geotechnik Graz*, Technische Universität Graz, Heft 8, 2000.

Kramer, J., and Semprich, S., Erfahrungen über den Druckluftverbrauch bei der Spritzbetonbauweise. *Tunnelbau-Taschenbuch, Verlag Glückauf, Essen*, 91-153, 1989.

Mualem, Y., A New Model for Predicting the Hydraulic Conductivity of Unsaturated Porous Media, *Water Resources Research*, 12(3), 513-522, 1980.

Pruess, K., Oldenburg, C., and Moridis, G., *TOUGH2 User's Guide 2.0*. Earth Sciences Division, Ernest Orlando Lawrence Berkeley National Laboratory, 1999.

Scheid, Y., Einfluß der Strömungsmechanik teilgesättigter Böden beim Tunnelbau unter Druckluft nach NATM, PhD-thesis, Institute for Soil Mechanics and Foundation Engineering, Graz University of Technology, 2003.

Steger, G., and Semprich, S., Tunnelbau unter Druck-luft- Numerische Ermittlung von Luftbedarfs-prognosen mit ASCATA., *Geotechnik*, 28 (4), 263-270, 2005.